JACS
JOURNAL OF THE AMERICAN CHEMICAL SOCIETY

Communication

pubs.acs.org/JACS

Multiple Orbital Effects and Magnetic Ordering in a Neutral Radical

Aaron Mailman,[†] Stephen M. Winter,[†] Joanne W. L. Wong,[†] Craig M. Robertson,[‡] Abdeljalil Assoud,[†] Paul A. Dube,[§] and Richard T. Oakley*,[†]

[†]Department of Chemistry, University of Waterloo, Waterloo, Ontario N2L 3G1, Canada

[‡]Department of Chemistry, University of Liverpool, Liverpool L69 7ZD, U.K.

[§]Brockhouse Institute for Materials Research, McMaster University, Hamilton, Ontario L8S 4M1, Canada

Supporting Information

ABSTRACT: The alternating ABABAB π-stacked architecture of the EtCN solvate of the iodo-substituted, oxobenzene-bridged bisdithiazolyl radical IBBO (space group *Pnma*) gives rise to strong ferromagnetic exchange along the π-stacks, and the material orders as a spin-canted antiferromagnet with T_N = 35 K, with a spontaneous (canted) moment M_{spont} = 1.4 × 10^{-3} μ_B and a coercive field H_c = 1060 Oe (at 2 K). The observation of spin-canting can only be understood in terms of multiorbital contributions to both isotropic and anisotropic exchange interactions, the magnitude of which are enhanced by spin−orbit effects arising from the heavy-atom iodine substituent. Pseudodipolar interactions lead to a net canted moment along the *c*-axis, while the sublattice magnetization is predicted to possess an easy *a*-axis.

Exploration of the charge transport[1] and magnetic[2] properties of organic radicals plays an important role in the understanding and development of strongly correlated materials. In light atom (N, O) radicals, such as nitroxyls and verdazyls, the intrinsically large on-site Coulomb repulsion *U* associated with electron hopping ensures a Mott insulating state.[3] Improvements in conductivity can be effected by using heavier *p*-block heteroatoms (S, Se), as their larger valence orbitals improve intermolecular overlap.[4] At the same time magnetic interactions are increased, and examples of S/Se-based radicals displaying ferromagnetic (FM) and spin-canted antiferromagnetic (AFM) order at temperatures above 10 K have been reported.[5] Magnetic interactions in these systems are dominated by isotropic exchange $\mathcal{H} = -2J_{ij}\mathbf{S}_i\cdot\mathbf{S}_j$, often described in terms of the two-site single orbital Hubbard model.[6] Accordingly the magnitude of the exchange energy J_{ij} between two radicals on adjacent sites (*i*,*j*) depends upon (i) the intermolecular hopping t_{ij}, which is directly related to the SOMO−SOMO overlap, (ii) the on-site Coulomb potential *U*, and (iii) electron exchange K_{ij} (Hund's coupling) between radicals.[7] Qualitatively, strong overlap leads to a large virtual hopping term $4(t_{ij})^2/U$, which favors AFM exchange (−ve *J*), while FM exchange (+ve *J*) is favored when SOMO−SOMO overlap, and hence t_{ij}, is nullified.[8]

While this one-orbital picture of the electronic and magnetic structure of radicals is appropriate in many cases, the importance of multiple orbital effects has recently been recognized in bisdithiazolyl (RBBO) radicals (Figure 1), where two dithiazolyl rings are bridged by an oxobenzene unit.[9] In such systems, the presence of carbonyl group does not perturb the SOMO, but mixing with the CO π^*-orbital lowers the energy of the LUMO and gives rise to a small SOMO−LUMO energy gap $\Delta\epsilon$.[10] The presence of the low-lying LUMO, in addition to large on-site SOMO−LUMO Hund's coupling K_{ii}^{01}, leads to strong ferromagnetic exchange interactions through virtual hopping processes,[11] an effect first recognized by Anderson[12] and Goodenough,[13] in the context of magnetic oxides. Their ideas were later applied to the design of ferromagnetic charge transfer salts[14] and doped fullerenes.[15] In this report we explore further the magnetic properties of the multiorbital RBBO radicals and examine the contributions to spin−orbit anisotropic exchange interactions associated with heavy R-substituents.

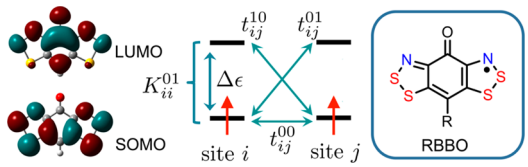

Figure 1. Frontier orbital interactions between two RBBO radicals (R = H) with a small SOMO−LUMO gap $\Delta\epsilon$. The SOMO−SOMO (t_{ij}^{00}) and SOMO−LUMO (t_{ij}^{10} and t_{ij}^{01}) hopping integrals and the SOMO−LUMO electron exchange integral K_{ii}^{01} are also defined.

Scheme 1

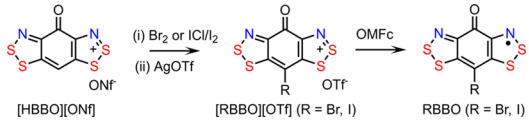

To this end we have extended the known halo-substituted radicals RBBO (R = F, Cl) to include the Br- and I-derivatives. Their preparation involves oxidation of the prototypal cation $[HBBO]^+$ with Br_2 or an ICl/I_2 mixture, respectively (Scheme 1). Reduction of the resulting bromo- and iodo-substituted cations with octamethylferrocene (OMFc) in MeCN affords the desired radicals, which crystallize from MeCN as 1:1 solvates that are isostructural (space group $Pna2_1$) with the previously reported ClBBO·MeCN.[16] In an attempt to avoid solvate formation, we repeated the preparation of the iodo-derivative IBBO using EtCN as solvent, an approach that was successful for R = Cl.[9] However,

Received: November 30, 2014
Published: January 14, 2015

DOI: 10.1021/ja512235h
J. Am. Chem. Soc. 2015, 137, 1044−1047

the radical still crystallized as a 1:1 solvate IBBO·EtCN, but with a space group (*Pnma*) and packing pattern different from that of the MeCN solvate. This new material displays remarkable magnetic properties.

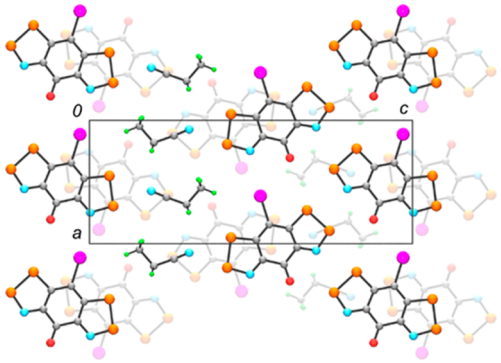

Figure 2. Unit cell of IBBO·EtCN (at 100 K), with ribbon-like arrays of radicals running parallel to the *a*-axis. Radicals at y = 0.25, 0.75 form centrosummetric ABABAB π-stacked arrays.

The crystal structure of IBBO·EtCN consists of IBBO radicals π-stacked in alternating ABABAB columns running parallel to the *b*-axis, with adjacent radicals along the stack related by a crystallographic inversion center (Figure 2). Each radical lies on a mirror plane normal to *b* at y = 0.25, 0.75, and is linked into ribbon-like arrays along the *a*-glide by close (inside van der Waals)[17] intermolecular S···N′, S···O′, and S···S′ interactions (see Supporting Information for numerical details). In addition, radicals related by translation along *a* are separated by short I···N′ and I···O′ contacts. The EtCN solvent molecule is aligned parallel to the plane of the radical and is locked onto one end by a pair of close EtCN···S′ contacts. Structurally, the solvent molecules serve as a buffer between adjacent ribbons and inhibit magnetic interactions between them.

Variable temperature, 4-probe conductivity measurements on IBBO·EtCN (Figure S1) afforded $\sigma(295\ \mathrm{K}) = 8.1 \times 10^{-4}$ S cm^{-1} and $E_{act} = 0.14$ eV, consistent with Mott insulating behavior. Initial field cooled variable temperature (2−300 K) magnetic susceptibility (χ) measurements at H = 1 kOe (Figure 3a) revealed strong FM exchange interactions, indicated by a Θ-value of +23.3 K extracted from a Curie−Weiss fit to the 100−300 K data (Figure S2). The subsequent decrease in χT on cooling below 90 K heralded the onset of weaker AFM interactions, which ultimately led to spin-canted antiferromagnetic ordering below T_N = 35 K, as indicated by bifurcation in χT for the zero-field cooled (ZFC) and field cooled (FC) sweeps. Field independent magnetization experiments (Figure 3b) supported this conclusion and established a spontaneous (canted) moment $M_{spont} = 1.4 \times 10^{-3}\ \mu_B$. Isothermal magnetization measurements indicated a weak, quasi-linear M vs H dependence out to 50 kOe. Cycling of the field revealed a hysteretic response in $M(H)$ (Figure 3c), with an associated coercive field H_c = 1060 Oe (at T = 2 K). Evidence for a relatively sharp spin-flop transition associated with easy-axis anisotropy can also be seen in the dM/dH curves (Figure 3d), which show a characteristic peak at H_{sf} = 21 kOe.

Low temperature (T = 28 K) X-ray diffraction measurements established that the transition to spin-canted antiferromagnetic order is not associated with a structural (space group) change. For this reason, the magnetic structure of IBBO·EtCN may be uniquely identified, as a net canted moment can only occur in simple two-sublattice antiferromagnets if sites related by either

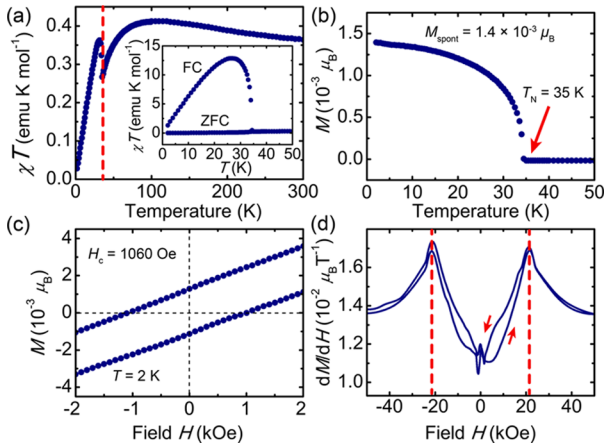

Figure 3. Magnetic measurements for IBBO·EtCN. (a) Field-cooled χT vs T plot at H = 1 kOe, with ZFC-FC plot of χT vs T at H = 10 Oe inset. (b) Decay in spontaneous magnetization M with temperature. (c) Hysteresis in cycling of M vs H at T = 2 K. (d) dM/dH curves over one hysteresis loop at T = 2 K, showing spin-flop transition near H_{sf} = 21 kOe.

translation or inversion belong to the same magnetic sublattice. In the *Pnma* space group, this condition is satisfied only for FM alignment of inversion-related spins on adjacent radicals in the same π-stack. By contrast, radicals related by the *a*-glide, coupled via lateral magnetic interactions, must be AFM aligned, as shown in Figure 4. The buffering effect of the solvent molecules ensures that J_π and J_{lat} are the only magnetic interactions of appreciable magnitude.[18] For this arrangement of spins, a canted moment may appear in the *ac*-plane.

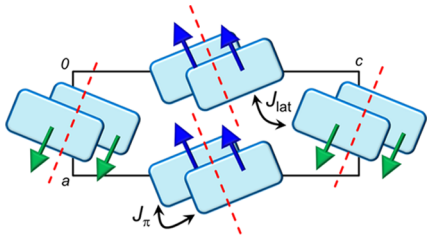

Figure 4. Magnetic structure of IBBO·EtCN, illustrating canting of spins to produce a net moment along the *c*-direction. Dashed lines indicate the orientation of the local easy axis associated with each π-stack arising from $\mathbf{\Gamma}_\pi^{FM}$. Pairwise exchange interactions J_π and J_{lat} are discussed in the text.

To analyze the magnetic response of IBBO·EtCN quantitatively, we begin by noting that for each radical pair (i,j), magnetic interactions may be described by the general Hamiltonian:

$$\mathcal{H}_{ij} = -2J_{ij}\mathbf{S}_i\cdot\mathbf{S}_j + \mathbf{D}_{ij}\cdot\mathbf{S}_i \times \mathbf{S}_j + \mathbf{S}_i\cdot\mathbf{\Gamma}_{ij}\cdot\mathbf{S}_j \quad (1)$$

where J_{ij} is the isotropic exchange constant, $\mathbf{D}_{ij}$ is the Dzyalloshinskii−Moriya vector, and $\mathbf{\Gamma}_{ij}$ is the symmetric pseudodipolar tensor. Including multiorbital effects, the first of these may be separated into FM and AFM contributions:

$$2J_{ij}^{AFM} = -4\frac{(t_{ij}^{00})^2}{U} \quad (2)$$

$$2J_{ij}^{FM} = 2K_{ij}^{00} + 2\frac{(t_{ij}^{01})^2 + (t_{ij}^{10})^2}{(V+\Delta\epsilon)^2 - (K_{ii}^{01})^2}K_{ii}^{01} \quad (3)$$

where t_{ij}^{ab} gives the hopping integral between orbital ϕ_i^a on site i and orbital ϕ_j^b at site j. Hund's rule coupling is described by the

DOI: 10.1021/ja512235h
J. Am. Chem. Soc. 2015, 137, 1044−1047

Coulomb integral K_{ij}^{ab}. There are two types of on-site Coulomb repulsion, namely, that between electrons in the same orbital (U) and different orbitals ($V < U$). For large t_{ij}^{01} and K_{ii}^{01}, and/or small $\Delta\epsilon$, the FM exchange is dominated by the second term in eq (3), representing the multiorbital enhancement of the effective intersite Hund's coupling, leading to FM interactions. On the basis of eqs (2) and (3), exchange energies corresponding to interactions along the π-stacks and along the ribbons, that is J_π and J_{lat} in Figure 4, were estimated from analysis of quantum chemistry calculations[19] described in the Supporting Information. The computed J_π and J_{lat} values (Table 1) increase on cooling, which may be related to contraction in the cell volume.[20] For the 28 K structure, $J_\pi = +140\ \text{cm}^{-1}$ and $J_{\text{lat}} = -28.1\ \text{cm}^{-1}$ were obtained. For the former interaction, the SOMOs are nearly orthogonal, with $t_\pi^{00} = 2.7$ meV, while strong SOMO−LUMO overlap ($t_\pi^{01} = t_\pi^{10} = 210$ meV) and large Hund's coupling $K_{ii}^{01} = 0.2$ eV favors FM interactions. Overall, the sign and magnitude of the computed exchange energies are consistent with (i) the magnetic structure shown in Figure 4, (ii) the large +ve Θ-value, and (iii) the high T_N value (to date, the second highest for a nonmetallic magnet).[5a]

Table 1. Cell Volume and Computed Magnetic Parameters

T (K)	Volume (Å^3)	J_π (cm^{-1})	J_{lat} (cm^{-1})	H_A (Oe)	H_{sf} (kOe)
28	1286.8(9)	+140	−28.1	711	22
100	1293.99(10)	+136	−20.8	732	23
293	1341.58(3)	+106	−19.9	502	19

Having described the isotropic interactions, we turn to the anisotropic terms in eq 1, which are responsible for both spin-canting and the magnetic hysteresis.[21,22] In Moriya's standard description,[23] such interactions arise as a modification of the AFM exchange due to spin−orbit coupling (SOC) effects:

$$\mathbf{D}_{ij}^{\text{AFM}} = \frac{4i}{U}\{t_{ij}^{00}\mathbf{C}_{ji}^{00} - \mathbf{C}_{ij}^{00}t_{ji}^{00}\} \tag{4}$$

$$\mathbf{\Gamma}_{ij}^{\text{AFM}} = \frac{4}{U}\{\mathbf{C}_{ij}^{00} \otimes \mathbf{C}_{ji}^{00} + \mathbf{C}_{ji}^{00} \otimes \mathbf{C}_{ij}^{00}\} \tag{5}$$

where Moriya's spin−orbit mediated hopping parameter $\mathbf{C}_{ij}^{00}$ is a (pseudo)vector given by

$$C_{ij}^{00} = \frac{1}{2}\sum_a \left\{ \frac{\mathcal{L}_i^{0a}}{\epsilon_a - \epsilon_0} t_{ij}^{0a} + t_{ij}^{0a} \frac{\mathcal{L}_j^{a0}}{\epsilon_a - \epsilon_0} \right\} \tag{6}$$

and $\mathcal{L}_i^{ab} = \langle \phi_i^a | \mathcal{L}_i | \phi_i^b \rangle$ denotes a matrix element of spin−orbit mean field angular momentum between orbitals ϕ_i^a and ϕ_i^b at radical site i. When SOC corrections to the FM exchange terms are considered, an anomalous symmetry $\mathbf{\Gamma}_{ij}^{\text{AFM}} \propto \mathbf{D}_{ij}^{\text{AFM}} \otimes \mathbf{D}_{ij}^{\text{AFM}}$ that appears in Moriya's description is broken.[24] This observation is important for IBBO·EtCN because *all* anisotropic contributions described by the conventional expressions (4) and (5) vanish for both π-stack and lateral interactions, as discussed below. Spin-canting and magnetic anisotropy can *only* emerge from multiorbital spin−orbit interactions, for which we introduce the expressions:

$$\mathbf{D}_{ij}^{\text{FM}} = 2i\left\{ \frac{\mathbf{C}_{ij}^{01}t_{ji}^{10} - t_{ij}^{10}\mathbf{C}_{ji}^{01}}{(V + \Delta\epsilon)^2 - (K_{ii}^{01})^2} \right\} K_{ii}^{01} \tag{7}$$

$$\mathbf{\Gamma}_{ij}^{\text{FM}} = -2\left\{ \frac{\mathbf{C}_{ij}^{01} \otimes \mathbf{C}_{ji}^{10} + \mathbf{C}_{ji}^{10} \otimes \mathbf{C}_{ij}^{10}}{(V + \Delta\epsilon)^2 - (K_{ii}^{01})^2} \right\} K_{ii}^{01} \tag{8}$$

where the interorbital spin−orbit mediated hopping is given by

$$\mathbf{C}_{ij}^{01} = \frac{1}{2}\sum_a \left\{ \frac{\mathcal{L}_i^{0a}}{\epsilon_a - \epsilon_0} t_{ij}^{a1} + t_{ij}^{0a} \frac{\mathcal{L}_j^{a1}}{\epsilon_a - \epsilon_0 + V} \right\} \tag{9}$$

These expressions are valid for the case of a single low-lying LUMO. The total quantities appearing in eq 1 are a sum of AFM and FM contributions, for example, $\mathbf{D}_{ij} = \mathbf{D}_{ij}^{\text{AFM}} + \mathbf{D}_{ij}^{\text{FM}}$.

For the lateral, ribbon-type interactions, *all* anisotropic terms described by eqs (4)−(9) are essentially vanishing. To see this, note that such radical pairs lie on a crystallographic mirror plane normal to the b-axis. Symmetry therefore dictates that $\mathbf{C}_{\text{lat}}^{00}$ is confined to lie parallel to b and depends only on the y-component of the angular momentum matrix elements denoted $[\mathcal{L}_i^{0a}]_y$. However, since $L_y|p_y\rangle = 0$, and the SOMO ϕ_i^0 is a π-orbital formed approximately from a linear combination of p_y orbitals centered at various atoms, it follows that $[\mathcal{L}_i^{0a}]_y \approx 0$ for all orbitals ϕ_i^a. In other words, SOC induces very little orbital angular momentum about the normal of the molecular plane. Thus, $\mathbf{C}_{\text{lat}}^{00} \approx 0$, a result that is confirmed by ab-initio calculations described below. The same argument requires that interorbital spin−orbit hopping $\mathbf{C}_{\text{lat}}^{01}$ and $\mathbf{C}_{\text{lat}}^{10} \approx 0$ since the LUMO ϕ_i^1 is also of p_y (π-type) composition, so that spin−orbit matrix elements $[\mathcal{L}_i^{1a}]_y$ associated with the LUMO are also small. Thus, both the AFM contributions $\mathbf{D}_{\text{lat}}^{\text{AFM}}$, $\mathbf{\Gamma}_{\text{lat}}^{\text{AFM}}$ and the FM contributions $\mathbf{D}_{\text{lat}}^{\text{FM}}$, $\mathbf{\Gamma}_{\text{lat}}^{\text{FM}}$ are negligible for the lateral interactions.

The observed magnetic anisotropy must therefore arise from nearest neighbor interactions *within* the π-stacks, that is, between molecules related by inversion. For these π-stacked radical pairs, all Dzyalloshinskii−Moriya interactions vanish, that is, $\mathbf{D}_\pi = \mathbf{D}_\pi^{\text{AFM}} = \mathbf{D}_\pi^{\text{FM}} = 0$ by symmetry, and $\mathbf{\Gamma}_\pi^{\text{AFM}} \propto \mathbf{D}_\pi^{\text{AFM}} \otimes \mathbf{D}_\pi^{\text{AFM}} = 0$ follows. The only remaining nonvanishing term is the multiorbital contribution $\mathbf{\Gamma}_\pi^{\text{FM}}$, which can be nonzero despite the presence of the inversion center. This represents the *only* source of magnetic anisotropy, and it is for this reason that IBBO·EtCN is uniquely suited for studying multiorbital anisotropic exchange.

To obtain a quantitative estimate of the anisotropic exchange terms, the required hopping integrals, spin−orbit matrix elements, and orbital energies were calculated on the basis of structures at 28 K, 100 K, and 296 K.[16] Spin−orbit hopping parameters $\mathbf{C}_{ij}$ were then computed from eqs (6) and (9). In agreement with the above discussion, the results suggest $|\mathbf{C}_{\text{lat}}^{00}|$, $|\mathbf{C}_{\text{lat}}^{01}|$, $|\mathbf{C}_{\text{lat}}^{10}| < 10^{-3}$ meV at all temperatures, while $|\mathbf{C}_\pi^{00}| = 0$ by symmetry. By contrast, $|\mathbf{C}_\pi^{01}| = |\mathbf{C}_\pi^{10}| = 3.4$ meV (at 28 K). The resulting pseudodipolar interaction $\mathbf{\Gamma}_\pi^{\text{FM}}$, computed via eq (8), provides each π-stack with a local easy axis that lies nearly along the a-axis, tilted 16° toward the c-axis. The direction of this tilt differs between magnetic sublattices, which gives rise to both a small net canted moment along the c-axis and an easy a-axis for the sublattice magnetization on average.

The magnitude of the anisotropy may be characterized in terms of the anisotropy field H_A (Table 1), estimated from the difference in energy for all spins aligned parallel to the easy a- and hard b-axes. By extrapolation of the magnetization, we find the saturation field of IBBO·EtCN to be $2H_E = 700$ kOe, from which it is possible to predict the spin-flop field $H_{sf} = (2H_E H_A)^{1/2}$, assuming pure uniaxial anisotropy. The calculated H_{sf} values (at different temperatures) fall within the range 19−23 kOe, which is

DOI: 10.1021/ja512235h
J. Am. Chem. Soc. 2015, 137, 1044−1047

satisfyingly close to the observed H_{sf} = 21 kOe (Figure 3d), a correspondence that substantiates the magnitude of the computed $\mathbf{\Gamma}_{\pi}^{FM}$ terms.

In summary we note that, in multiorbital radicals, the strength of various spin−orbit terms may be controlled by rational functionalization of the organic building block. A large spin−orbit mixing of any two orbitals ϕ_i^a and ϕ_i^b requires that both have density on a common heavy element ($n > 3$). While Moriya's conventional anisotropic exchange (eq (4)−(6)) depends only on spin−orbit corrections to the SOMO, quantified by $\mathcal{L}_i^{0a}$ matrix elements, multiorbital anisotropic exchange depends also on modifications to the LUMO through $\mathcal{L}_i^{1a}$ matrix elements. In IBBO·EtCN, these latter terms are enhanced by the presence of the heavy iodine substituent, which provides a nonzero coefficient for the iodine $5p_{\pi}$-orbital in the LUMO. Large magnetic anisotropy therefore arises directly from the basal substituent. In contrast, spin−orbit effects associated with the SOMO are relatively independent of the R-group, due to the presence of a nodal plane in the SOMO (Figure 1). In this way, it may be seen that anisotropy in magnetically active radicals may be generated either by the direct incorporation of heavy atoms into spin-bearing sites, as previously demonstrated,[5d] or indirectly through modification of multiorbital FM contributions by introduction of heavy atoms into non-spin-bearing sites, as shown here.

■ ASSOCIATED CONTENT

Supporting Information

Experimental and computational details and structural characterization data. This material is available free of charge via the Internet at http://pubs.acs.org.

■ AUTHOR INFORMATION

Corresponding Author

*oakley@uwaterloo.ca

Notes

The authors declare no competing financial interest.

■ ACKNOWLEDGMENTS

We thank the Natural Sciences and Engineering Research Council of Canada for financial support, and the Diamond Light Source for access to beamline I19.

■ REFERENCES

(1) (a) Haddon, R. C. *Nature* **1975**, *256*, 394. (b) Haddon, R. C. *ChemPhysChem* **2012**, *13*, 3581. (c) Awaga, K.; Nomura, K.; Kishida, H.; Fujita, W.; Yoshikawa, H.; Matsushita, M. M.; Hu, L.; Shuku, Y.; Suizu, R. *Bull. Chem. Soc. Jpn.* **2014**, *87*, 234.

(2) (a) Kinoshita, M. In *π-Electron Magnetism: From Molecules to Magnetic Materials*; Veciana, J., Arcon, D., Eds.; Springer: Berlin, Germany, 2001; Chapter 1. (b) Ratera, I.; Veciana, J. *Chem. Soc. Rev.* **2012**, *41*, 303. (c) Lahti, P. *Adv. Phys. Org. Chem.* **2011**, *45*, 93. (d) Rawson, J. M.; Alberola, A.; Whalley, A. *J. Mater. Chem.* **2006**, *16*, 2560.

(3) Mott, N. F. *Proc. Phys. Soc., London, Sect. A* **1949**, *62*, 416.

(4) (a) Hicks, R. G. In *Stable Radicals: Fundamentals and Applied Aspects of Odd-Electron Compounds*; Hicks, R. G., Ed.; John Wiley & Sons, Ltd.: Wiltshire, U.K., 2010; pp 317−380. (b) Brusso, J. L.; Cvrkalj, K.; Leitch, A. A.; Oakley, R. T.; Reed, R. W.; Robertson, C. M. *J. Am. Chem. Soc.* **2006**, *128*, 15080.

(5) (a) Banister, A. J.; Bricklebank, N.; Lavender, I.; Rawson, J. M.; Gregory, C. I.; Tanner, B. K.; Clegg, W.; Elsegood, M. R. J.; Palacio, F. *Angew. Chem., Int. Ed.* **1996**, *35*, 2533. (b) Leitch, A. A.; Brusso, J. L.; Cvrkalj, K.; Reed, R. W.; Robertson, C. M.; Dube, P. A.; Oakley, R. T. *Chem. Commun.* **2007**, 3368. (c) Robertson, C. M.; Leitch, A. A.; Cvrkalj, K.; Reed, R. W.; Myles, D. J. T.; Dube, P. A.; Oakley, R. T. *J. Am. Chem. Soc.* **2008**, *130*, 8414. (d) Winter, S. M.; Oakley, R. T.; Kovalev, A. E.; Hill, S. *Phys. Rev. B* **2012**, *85*, 094430.

(6) Hubbard, J. *Proc. R. Soc. (London)* **1963**, *A276*, 238.

(7) Calzado, C. J.; Cabrero, J.; Malrieu, J. P.; Caballol, R. *J. Chem. Phys.* **2002**, *116*, 2728.

(8) Kahn, O.; Galy, J.; Journaux, Y.; Jaud, J.; Morgenstern-Badarau, I. *J. Am. Chem. Soc.* **1982**, *104*, 2165.

(9) Yu, X.; Mailman, A.; Lekin, K.; Assoud, A.; Robertson, C. M.; Noll, B. C.; Campana, C. F.; Howard, J. A. K.; Dube, P. A.; Oakley, R. T. *J. Am. Chem. Soc.* **2012**, *134*, 2264.

(10) (a) Wong, J. W. L.; Mailman, A.; Lekin, K.; Winter, S. M.; Yong, W.; Zhao, J.; Garimella, S. V.; Tse, J. S.; Secco, R. A.; Desgreniers, S.; Ohishi, Y.; Borondics, F.; Oakley, R. T. *J. Am. Chem. Soc.* **2014**, *136*, 1070. (b) Wong, J. W. L.; Mailman, A.; Winter, S. M.; Robertson, C. M.; Holmberg, R. J.; Murugesu, M.; Dube, P. A.; Oakley, R. T. *Chem. Commun.* **2014**, *50*, 785.

(11) (a) Mailman, A.; Winter, S. M.; Yu, X.; Robertson, C. M.; Yong, W.; Tse, J. S.; Secco, R. A.; Liu, Z.; Dube, P. A.; Howard, J. A. K.; Oakley, R. T. *J. Am. Chem. Soc.* **2012**, *134*, 9886. (b) Winter, S. M.; Mailman, A.; Oakley, R. T.; Thirunavukkuarasu, K.; Hill, S.; Graf, D. E.; Tozer, S. W.; Tse, J. S.; Mito, M.; Yamaguchi, H. *Phys. Rev. B* **2014**, *89*, 214403.

(12) Anderson, P. W. *Phys. Rev.* **1959**, *115*, 2.

(13) Goodenough, J. B. *J. Phys. Chem. Solids* **1958**, *6*, 287.

(14) (a) Williams, K. A.; Nowak, M. J.; Dormann, E.; Wudl, F. *Synth. Met.* **1986**, *14*, 233. (b) Miller, J. S.; Epstein, A. J.; Reiff, W. M. *Chem. Rev.* **1988**, *88*, 201. (c) Fujita, W.; Awaga, K. *Chem. Phys. Lett.* **2004**, *388*, 186. (d) Fujita, W. *Dalton Trans.* **2015**, *44*, 903.

(15) (a) Allemand, P. M.; Khemani, K. C.; Koch, A.; Wudl, F.; Holczer, K.; Donovan, S.; Gruner, G.; Thompson, J. D. *Science* **1991**, *253*, 301. (b) Arovas, D. P.; Auerbach, A. *Phys. Rev. B* **1995**, *52*, 10114.

(16) Details of the crystal structures of RBBO·MeCN (R = Br, I) and of IBBO·EtCN at 296 K, 100 K, and 28 K are provided in the Supporting Information. Crystallographic information files are available through the Cambridge Crystallographic Data Centre, reference numbers CCDC-103-5855 to CCDC-103-5859.

(17) Bondi, A. *J. Phys. Chem.* **1964**, *68*, 441.

(18) There is a third interaction between radicals related by translation along *a*; calculations suggest these are weakly FM, with $J < 3$ cm^{-1}, and make no contribution to the anisotropy.

(19) (a) Neese, F. *Wiley Interdiscip. Rev. Comput. Mol. Sci.* **2012**, *2*, 73. (b) Hess, B. A.; Marian, C. M.; Wahlgren, U.; Gropen, O. *Chem. Phys. Lett.* **1996**, *251*, 365.

(20) Veber, S. L.; Fedin, M. V.; Potapov, A. I.; Maryunina, K. Y.; Romanenko, G. V.; Sagdeev, R. Z.; Ovcharenko, V. I.; Goldfarb, D.; Bagryanskaya, E. G. *J. Am. Chem. Soc.* **2008**, *130*, 2444.

(21) Anisotropy may also arise from classical dipolar effects, which may be estimated from computed spin densities. This approach works well for nitroxyls (ref 22), where $H_A \lesssim 100$ Oe, but in the present case dipolar terms, associated with an easy *b*-axis, likely represent a small (∼10%) correction to the spin−orbit contribution to H_A.

(22) (a) Stanger, J.-L.; Andre, J.-J.; Turek, P.; Hosokoshi, Y.; Tamura, M.; Kinoshita, M.; Rey, P.; Cirujeda, J.; Veciana, J. *Phys. Rev. B* **1997**, *55*, 8398. (b) Kajiyoshi, K.-I.; Kambe, T.; Tamura, M.; Oshima, K. *J. Phys. Soc. Jpn.* **2006**, *75*, 074702.

(23) (a) Moriya, T. *Phys. Rev.* **1960**, *120*, 91. (b) Dzyaloshinsky, I. *J. Phys. Chem. Solids* **1958**, *4*, 241.

(24) Yildirim, T.; Harris, A. B.; Aharony, A.; Entin-Wohlman, O. *Phys. Rev. B* **1995**, *52*, 10239.

DOI: 10.1021/ja512235h
J. Am. Chem. Soc. 2015, 137, 1044−1047